Solid-State Electronics 186 (2021) 108169

Contents lists available at ScienceDirect

Solid State Electronics

journal homepage: www.elsevier.com/locate/sse

Express method of electro-physical parameters extraction for power Schottky diodes

Vasily A. Krasnov, Sergey Yu. Yerochin *, Oleksii M. Demenskyi

V. Lashkaryov Institute of Semiconductor Physics, National Academy of Sciences of Ukraine, Laboratory of Materials for Optoelectronics N10-2, Kherson 73008, Ukraine

ARTICLE INFO

The review of this paper was arranged by Prof. S. Cristoloveanu

Keywords:
Parameter extraction
Power semiconductor devices
Schottky diode
Silicon carbide
Characterization
High-voltage devices

ABSTRACT

A detailed express procedure of basic electro-physical parameters determination for power Schottky diodes has been presented. The procedure was approved using commercial diodes based on 4H-SiC by CREE, Inc. It relies on the device physical model only and almost excludes the usage of experimental data as the initial calculation parameters. During the calculation procedure the information available in the device datasheet is mainly used. If necessary, it may be supplemented by simple *C-V* and *I-V* characterization data of the device. The calculation technique is remarkable for its ability to extract electro-physical parameters of Schottky diodes with high accuracy and reliability. This is due to both: the usage of analytical equations instead of mathematical processing of the device characterization data presented graphically as well as the implementation of reliability control of obtained electro-physical parameters by calculating on their basis already known characteristics and parameters given in the datasheet or in the literature. The results of this work could promote the development of power Schottky and p-i-n diode operation theory at high temperatures.

1. Introduction

It is well known that unique electrical and electro-physical properties as well as thermal characteristics enable silicon carbide to be a promising semiconductor material for various designs of power semiconductor devices [1]. The application of SiC diodes, in particular, in gating circuits is considered to allow achieving high rates of power switching and operation performance [2,3].

In the issues of development and application of power Schottky diodes (SD) it is important to establish the connection between output characteristics of the device given in the datasheet and electro-physical parameters of semiconductor structure of the device. Such correlations usually are not cited in the datasheet and even if they are, the amount of data published is minimal. Nevertheless we believe that there are at least three considerable practical problems which demand knowing these correlations. The problems are: device and device structure characterization at the stage of development of physical and engineering solutions; study of mechanisms of the device parameter degradation due to long-term exploitation in the conditions of high voltages and currents, hard commutation modes and environmental exposure; recently emerged task of a device electro-physical parameter extraction based on physical simulation and using the data from datasheets and additional *I-V*, *C-V* and other device characterization techniques [4–10]. The information extracted is useful for both the development of applied-physics and schematic solutions as well as the disclosure of new device applications even having no concern with its direct function. In particular, the latter will be demonstrated below.

Known practical techniques of the device parameter extraction and experimental-theoretical procedures for determination of correlation dependency of device output characteristics on electro-physical parameters of its active structure (see, for example, [5]) possess some drawbacks. They are: a limitation of the parameters simulated and wide usage of empirical input data which narrows significantly the scope of a physical model chosen as well as the calculation procedures based on it.

In this work we propose an advanced technique of determination of electro-physical parameters of power SD active device structures, which includes the elements of physical modelling of the structure operation, the calculation of its electro-physical parameters and, in some cases, *I-V* and *C-V* characterization if the parameters needed are absent in the device datasheet[a]. The approval of theoretical and calculation results

* Corresponding author.
E-mail address: serger@isp.kiev.ua (S.Yu. Yerochin).

[a] We should note that method proposed cannot be applied "as is" to merged p-i-n SD [13,14]. In this case some modification is needed which is not the subject of present work.

https://doi.org/10.1016/j.sse.2021.108169
Received 23 February 2021; Received in revised form 19 June 2021; Accepted 12 August 2021
Available online 15 August 2021

was done for commercial power SiC Schottky diodes C3D02060E and C3D04060A [11,12] by Cree Inc., world leading developer of the power semiconductor SiC-based diodes.

2. The technique of diode parameter determination

The technique of power SD parameters determination proposed includes the following sequence of steps to be executed.

2.1. General analysis of the diode model

The simplified cross-section of the diode structure is given in Fig. 1.

The physical model of a SD implies the current flow mechanism in the active structure dominated by over-barrier thermionic emission of electrons being the majority charge carriers in the structures investigated [15,16]. In addition, as it follows from Poisson equation for the given structure [17], if the reverse voltage V applied to the structure is such that $V \leq V_{PT}$, where V_{PT} is the punch-through voltage (the voltage at which a low-doped drift region of the structure is fully depleted), then the electric field distribution is linear within the drift region (Fig. 2).

According to the model accepted it is assumed in our calculations that the following conditions are fulfilled: $N_D \approx n$ and $n \ll n^+$, where N_D is the doping level of the diode base by donor impurity, n and n^+ are the concentrations of electrons in the base area and in the low-resistant substrate correspondingly. The ideality factor of the diode I-V characteristic makes $m \approx 1.0$–1.03 [18].

Our advanced technique developed includes the procedures of determination of the following electro-physical parameters of active diode structures:

$R_d(T)$ – the dependence of a drift region resistance on the temperature T;

$n = N_D$ – the electrons concentration in the drift region (n), doping level in the diode base (N_D);

μ_n(300 K) – the electron mobility in the drift region at 300 K under the action of weak electric field;

$\mu_n(T)$ – the dependence of electron mobility on the temperature in the drift region at $T >$ 300 K under the action of weak electric fields;

$\mu_n(T_i)$ – the electron mobility value at $T = T_i$, where T_i is the estimated value of limiting operation temperature of the diode, i.e. the temperature of transition to the intrinsic conductivity state in the diode base area under the action of weak electric field;

L_D – the drift region width in the diode base area;

S – the active area of the diode structure;

Φ_B – metal-semiconductor Schottky barrier height;

A^* – the effective Richardson constant;

ΔT_h – the overheating temperature of diode active region at given

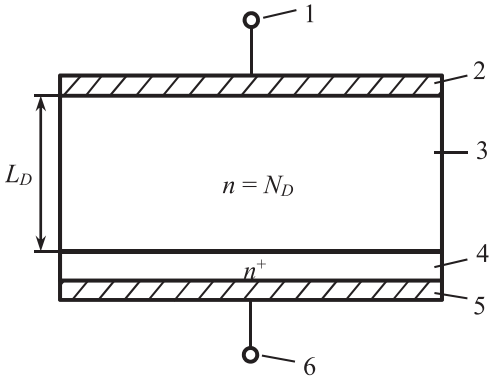

Fig. 1. The simplified structure of power Schottky diode Me–n-SiC used for the calculations: 1– the anode terminal; 2 – the actual anode; 3 – the drift region, n-4H-SiC; 4 – the substrate, 4H-n$^+$-SiC; 5 – the actual cathode; 6 – the cathode terminal.

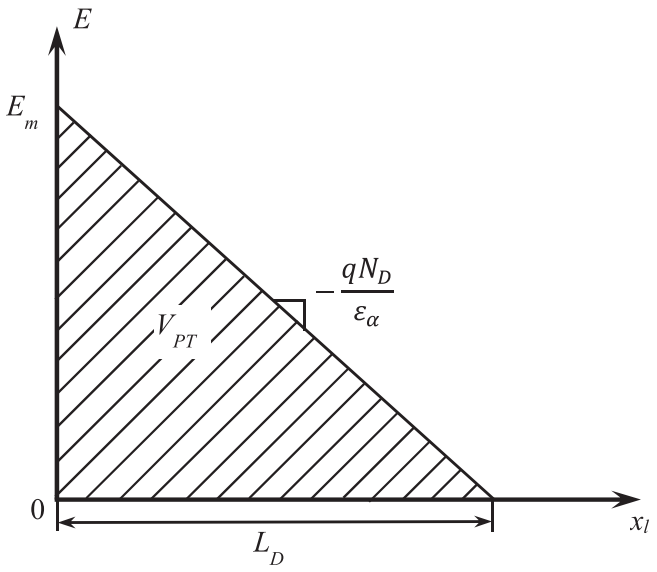

Fig. 2. Thickness distribution of electric field intensity E within a drift region x_l of the diode structure: E_m is the maximum value of electric field intensity.

forward voltage drop on the diode and/or forward current through it as well as given ambient temperature;

s and T_M – the thermometric characteristic parameters: thermal sensitivity and maximum measured temperature correspondingly – to be determined when transmitting "standard" operation current 10^{-5} A through the diode [19].

2.2. Determination of the temperature dependence of a drift region resistance R_d of the diode structure

For this purpose one can use a family of diode forward I-V characteristics measured at the chip temperature > 300 K in a pulse quasi-static mode with low duty cycle and short pulse duration applied to the diode (see, for example, [20]). When the applied voltage is $V > \Phi_B/q$, where q is the electron charge, then these characteristics are quasi-linear and could be given by:

$$V = V_0 + R_d(T_j)I, \tag{1}$$

where V_0 is the diode "cutoff" voltage, determined at the intersection of I-V line extension with the voltage axis, T_j is the diode chip temperature being equal to the ambient temperature, I is the diode forward current.

The values of $R_d(T)$ are proportional to the slope of dependencies (1). We should note that the linear behavior of (1) does not testify to the linearity of $R_d(T)$ dependence. However, in case of 4H-SiC SD chosen for the theory approval [11,12], as well as in case of other similar devices, the expression for $R_d(T)$ is satisfactorily fitted by the following linear relation in the wide temperature range $T \geq$ 300 K:

$$R_d(T) = R_0 + \alpha_R T \tag{2}$$

where R_0 is the constant, α_R is the temperature coefficient of R_d, $\alpha_R > 0$, 300 K $\leq T \leq T_i$.

The calculated values of parameters R_0, α_R, R_d(300 K) and $R_d(T)$

Table 1
Temperature dependence of a drift region resistance.

Device type	R_0, Ohm	α_R, Ohm/K	$R_d(T)$, Ohm	R_d(300 K), Ohm
C3D04060A	–0.158	8.3×10^{-4}	$-0.158 + 8.3 \times 10^{-4}$T	0.091
C3D02060E	–0.257	1.71×10^{-3}	$-0.257 + 1.71 \times 10^{-3}$T	0.256

expression for the diodes C3D04060A and C3D02060E are given in the Table 1.

2.3. C-V characterization of the diodes at a reverse bias

The characterization was done at the frequencies $f \geq 1$ MHz and voltages $|V| \leq V_{RSM}$, where V_{RSM} is the diode surge peak reverse voltage. The temperature was 300 K and the AC test signal amplitude was ~ 20 ÷ 25 mV.

The dependencies are given in the datasheets of diodes C3D02060E and C3D04060A (datasheet Figs. 4 and 6, correspondingly) [11,12].

2.4. Characterization of the punch-through parameters V_{PT} and C_{PT}

C_{PT} is the barrier capacity of the diode structure when $V = V_{PT}$. V_{PT} and C_{PT} are the coordinates of the intersection point of descending C-V curve and straight line $C = C_{PT} =$ const. on the C-V plot measured at a reverse bias [11,12].

C3D04060A: $V_{PT} \approx 200$ V, $C_{PT} \approx 15.15$ pF;

C3D02060E: $V_{PT} \approx 130$ V, $C_{PT} \approx 11.35$ pF.

2.5. Determination of N_D:

Using physical interpretation of the punch-through voltage, one can write the expression for dielectric relaxation time of charge carriers:

$$R_d C_{PT} = \varepsilon_\alpha \rho_D \tag{3}$$

where ε_α is the absolute permittivity of a semiconductor material in a drift region of the diode base layer, $\varepsilon_\alpha = \varepsilon_0 \varepsilon$, ε is the relative permittivity of a semiconductor, ε_0 is the permittivity of vacuum, ρ_D is the resistivity of a semiconductor material in a drift region of the diode base layer.

$$\rho_D = \frac{1}{\sigma_D}, \tag{4}$$

where σ_D is the conductivity of a semiconductor material in a drift region of the diode base layer.

Taking into account the condition of full impurity ionization in the low-doped region of the diode base ($n \approx N_D$), σ_D may be written as follows:

$$\sigma_D = q N_D \mu_n \tag{5}$$

Inserting (5) into (4) and then (4) into (3) let us express it in terms of the product $N_D \mu_n(N_D, 300\ \mathrm{K})$:

$$N_D \mu_n(N_D, 300K) = \frac{\varepsilon_\alpha}{q R_d(300K) C_{PT}} \tag{6}$$

Let's use approved in the art dependence of electron mobility on its concentration in low-doped 4H-SiC at 300 K and under low electric field [21,22]:

$$\mu_n(N_D, 300K) = \frac{\mu_{max} N_D}{1 + \left(\frac{N_D}{N_{ref}}\right)^\gamma} \tag{7}$$

where μ_{max}, N_{ref} and γ are the constants: $\mu_{max} = 1071\ \mathrm{cm^2/(V{\cdot}s)}$, $N_{ref} = 1.94 \times 10^{17}\ \mathrm{cm^{-3}}$, $\gamma = 0.4$.

Considering (6), equation (7) can be rewritten as follows:

$$\frac{\varepsilon_\alpha}{q R_d(300K) C_{PT}} = \frac{\mu_{max} N_D}{1 + \left(\frac{N_D}{N_{ref}}\right)^\gamma} \tag{8}$$

By solving transcendental equation (8) we obtained the value of N_D:

For C3D04060A: $N_D \approx 4.45 \times 10^{15}\ \mathrm{cm^{-3}}$, for C3D02060E: $N_D \approx 2.15 \times 10^{15}\ \mathrm{cm^{-3}}$.

2.6. Calculating of μ_n(300 K)

Using equation (6) we calculated μ_n(300 K):

$$\mu_n(300K) = \frac{\varepsilon_\alpha}{q R_d(300K) C_{PT} N_D} \tag{9}$$

For C3D04060A: μ_n(300 K) ≈ 875 $\mathrm{cm^2/V{\cdot}s}$, for C3D02060E: μ_n(300 K)≈ 925 $\mathrm{cm^2/V{\cdot}s}$.

2.7. Calculating of T_i

T_i is the limiting temperature value at which the intrinsic conductivity state occurs in the diode base layer. We assume that the value of T_i satisfy the criterion $n_i(T_i) \approx 0.1 N_D$ [23], where $n_i(T_i)$ is the intrinsic charge carriers concentration at $T = T_i$. The value of T_i is determined by solving the following transcendental equation:

$$(0.1N_D)^2 = N_C(T_i) N_V(T_i) exp\left[\frac{E_g(T_i)}{k_B T_i}\right], \tag{10}$$

or:

$$T_i = \frac{E_g(T_i)}{k_B ln\left[\frac{N_C(T_i) N_V(T_i)}{(0.1N_D)^2}\right]}, \tag{10a}$$

where $N_C(T_i)$, $N_V(T_i)$ are the effective density of states of electrons and holes respectively, at $T = T_i$, $E_g(T_i)$ is the energy band gap of the semiconductor in the diode base region at $T = T_i$, k_B is the Boltzman constant.

As for 4H-SiC, the relations for $N_C(T_i)$, $N_V(T_i)$ and $E_g(T_i)$ (in the form of Varshni formula) are written as follows [24]:

$N_C(T_i) = 3.25 \times 10^{15} T_i^{\frac{3}{2}}, N_V(T_i) = 4.85 \times 10^{15} T_i^{\frac{3}{2}}$, $\mathrm{cm^{-3}}$

$E_g(T_i) = 3.26 - 6.5 \times 10^{-4} \bullet \frac{T_i^2}{T_i + 1300}$, eV.

Calculated values of T_i and $E_g(T_i)$ for the device structures of C3D04060A and C3D02060E diodes are:

$T_i \approx 1290$ K, $E_g(T_i) \approx 2.842$ eV for C3D04060A, $T_i \approx 1200$ K, $E_g(T_i) \approx 2.886$ eV for C3D02060E.

2.8. Plotting of $\mu n(T)$ dependence

The dependence $\mu_n(T)$ in temperature range T > 300 K is usually plotted in the following form [22]:

$$\mu_n(T) = \mu_n(300K) \bullet \left(\frac{\mathrm{T}}{300}\right)^{-\mathrm{x}}, \tag{11}$$

Here we assume that the dependence $R_d(T)$ keeps its linear behavior in the whole range of temperatures investigated, i.e. 300 K ≤ $T \leq T_i$ [25]. Therefore we determine the value of exponent x using (11) and the following trivial relation for the mobilities:

$$\frac{R_d(T_i)}{R_d(300K)} = \frac{N_D \mu_n(300K)}{N_D(T_i) \mu_n(T_i)}, \tag{12}$$

After the transformations we obtain:

$$\frac{N_D(T_i)}{N_D} \bullet \frac{\mathrm{R_d(T_i)}}{\mathrm{R_d(300K)}} = \left(\frac{\mathrm{T_i}}{300}\right)^{\mathrm{x}}. \tag{12a}$$

Applying the above mentioned technical criterion $n_i(T_i) \approx 0.1 N_D$ and considering that $N_D(T_i) \approx N_D + 0.1 N_D$ we can rearrange (12a) in the form:

$$\frac{N_D + 0.1N_D}{N_D} \bullet \frac{\mathrm{R_d(T_i)}}{\mathrm{R_d(300K)}} \approx \left(\frac{\mathrm{T_i}}{300}\right)^{\mathrm{x}},$$

or:

$$\frac{1.1 R_d(T_i)}{R_d(300K)} \approx \left(\frac{T_i}{300}\right)^x, \tag{12b}$$

from which we obtain:

$$x = \frac{lg\left[\frac{1.1R_d(T_i)}{R_d(300K)}\right]}{lg\left(\frac{T_i}{300}\right)}. \quad (13)$$

For the structures of tested diodes the calculated values of x and $\mu_n(T_i)$ are as follows:

C3D04060A: $x \approx 1.64$, $\mu_n(T_i) \approx 80$ cm^2/(V·s); C3D02060E: $x \approx 1.47$, $\mu_n(T_i) \approx 120.8$ cm^2/(V·s).

Commentary. The values of × obtained testify to the current flow mechanism is dominated by charge carrier scattering by impurity ions ($\mu \sim T^{3/2}$ [26]) under given conditions. When the temperature rises, the carrier's mobility decreases. Moreover in the temperature range near T_i, the mobility also decreases at the expense of charge carrier concentration increase [15], which also increases the scattering effect. Note, that the values of $\mu_n(T_i)$ for these devices are approximately by an order of magnitude lower than those at $T = 300$ K (see above).

2.9. Calculation of L_D

The punch-through effect in the diode base region is achieved when the absolute value of reverse diode voltage equals V_{PT}. Considering this effect, the value of L_D can be found using the following formula, which takes into account triangular profile of the electric field distribution in the diode drift region:

$$L_D = \sqrt{\frac{2\varepsilon_\alpha V_{PT}}{qN_D}}, \quad (14)$$

C3D04060A: $L_D \approx 7.0$ μm; C3D02060E: $L_D \approx 8.3$ μm.

2.10. Calculation of S

a) By using the values of C_{PT} and L_D:

$$S = \frac{C_{PT}L_D}{\varepsilon_\alpha}, \quad (15)$$

C3D04060A: $S \approx 1.44$ mm^2; C3D02060E: $S \approx 1.1$ mm^2.

b) By using the values of L_D, μ_n(300 K), N_D and R_d(300 K):

$$S = \frac{L_D}{q\mu_n(300K)N_D R_d(300K)}, \quad (16)$$

C3D04060A: $S \approx 1.44$ mm^2; C3D02060E: $S \approx 1.1$ mm^2.

2.11. Calculation of the diffusion potential value V_{bi} for the Me-semiconductor junction

Using capacity-voltage characteristics $C(V)$ of the devices we find the diode capacitance at zero bias $C(0) = C_0$. Knowing C_0 one can find the thickness of the diode structure depletion region (W_0) at zero bias:

$$W_0 = \frac{\varepsilon_\alpha S}{C_0}. \quad (17)$$

It is known [15], that the value of W_0 is related to V_{bi} as follows:

$$W_0 = \left[\frac{2\varepsilon_\alpha}{qN_D}\left(V_{bi} - \frac{k_B T}{q}\right)\right]^{\frac{1}{2}}, \quad (18)$$

from which we obtain:

$$V_{bi} = \frac{qN_D W_0^2}{2\varepsilon_\alpha} + \frac{k_B}{q}, \quad (18a)$$

The value of V_{bi} can be determined graphically using the dependence $1/C^2 = f(V)$ plotted for the reverse biased diode [15]. However our studies have shown that the analytical method considered better correlates with the whole set of parameters being calculated.

C3D04060A: $W_0 \approx 0.5$ μm, V_{bi}(300 K) ≈ 1.07 V; C3D02060E: $W_0 \approx 0.7$ μm, V_{bi}(300 K) ≈ 1.01 V.

2.12. Determination of Φ_B

To calculate the value of Φ_B we have used the relation approved, particularly, in the work [27]:

$$\Phi_B = qV_{bi} + \frac{k_B T}{q} + \frac{k_B T}{q} ln\left[\frac{N_C(T)}{N_D}\right], T = 300\text{K} \quad (19)$$

C3D04060A: $\Phi_B \approx 1.3$ eV; C3D02060E: $\Phi_B \approx 1.26$ eV.

Further steps necessary to determine the desired parameters demand the measurements of current–voltage (*I-V*) characteristic of the diode at low current. We should note that such characteristics usually are not given in the device datasheet.

I-V characteristics of the diodes presented in this work were measured at 300 K in the range of currents $10^{-9} \div 1.0$ A and at forward voltage ≤ 1.25 V. The automated metrological test unit UGT-A [28] was used. The unit has the capability to carry out characterization in both: DC current mode and pulse quasi-static current mode. Absolute measurement error was no more than ~ 1.5 %.

I-V characterization data are shown in Figs. 3 and 4. The averaged value of ideality factor *m* obtained from the *I-V* data analysis was close to $m \approx 1.02 \div 1.03$. This may be connected with the influence of image

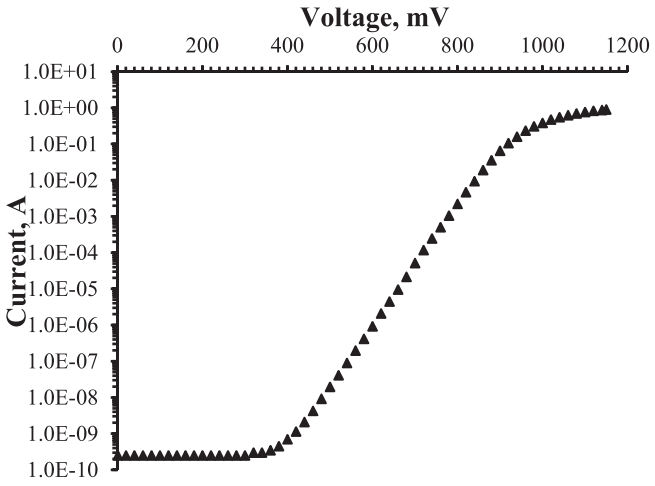

Fig. 3. *I-V* characteristic of the SD C3D02060E measured in the range of forward currents ~ 10^{-9}–1.0 A, T = 300 K.

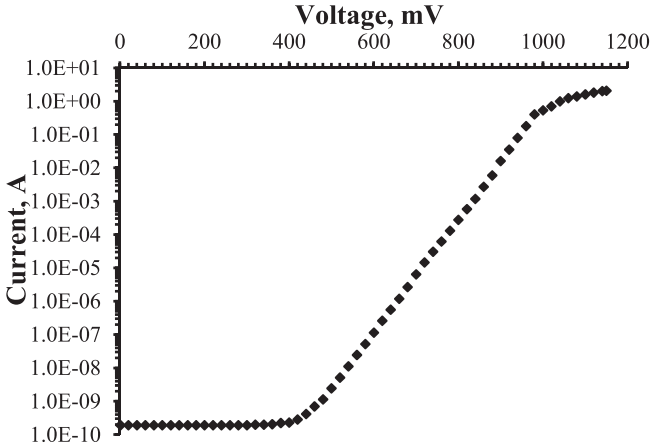

Fig. 4. *I-V* characteristic of the SD C3D04060A measured in the range of forward currents ~ 10^{-9}–1.0 A, T = 300 K.

forces and other factors on the height of metal–semiconductor potential barrier [15].

The experimental *I-V* curves behavior testifies to that the current flowing mechanism is dominated by over-barrier thermionic emission, which confirms our above assumptions (see Subsection 2.1).

Thermionic emission theory predicts the following dependence of the current on the applied voltage for SD:

$$I = I_S\left[exp\left(\frac{qV}{k_BT}\right) - 1\right], \tag{20}$$

$$I_S = SA^*T^2exp\left(-\frac{\Phi_{BC}}{k_BT}\right), \tag{20a}$$

where I_S is the saturation current, Φ_{BC} is the height of Me-semiconductor Schottky barrier, which is considered to be constant in the theory. Thus hereinafter we assume that $\Phi_{BC} = \Phi_B \approx$const.

The exponential section of *I-V* characteristic (see Figs. 3, 4) is satisfactorily approximated by the following dependence:

$$I = I_Sexp\left(\frac{qV}{mk_BT}\right), \tag{21}$$

where I_S is the coefficient being interpreted as a saturation current and corresponding to the relation [18]:

$$I_S = SA^*T^2exp\left(-\frac{\Phi_B}{k_BT}\right), \tag{21a}$$

2.13. The calculation of I_{lm}

I_{lm} is the maximum current at the "linear" section of dependence ln $I = f(V)$ (see the *I-V* characteristics in Figs. 3 and 4). We calculate I_{lm} using the natural condition of equality between ohmic resistance of the drift region and the diode differential resistance at a given temperature. It is assumed that the diode chip temperature equals the ambient temperature (in the thermostat) at the point $I_{lm}(V)$ during *I-V* characterization [20]:

$$I_{lm} = \frac{mk_BT_j}{qR_d(T_j)}, \tag{22}$$

C3D04060A: $I_{lm} \approx$0.286 A; C3D02060E: $I_{lm} \approx$0.1 A.

2.14. The calculation of I_S

We find the value of I_S by extrapolating the exponential section of *I-V* curve up to the value $V = mkT_j/q$ and by using the following relation for ideality factor *m*:

$$m \approx \frac{q\left[V_T\left(T_j, I_{lm}\right) - \frac{mk_BT_j}{q}\right]}{k_BT_jln\left(\frac{I_{lm}}{I_S}\right)}, \tag{23}$$

where $V_T(T_j, I_{lm})$ is the voltage on *I-V* curve corresponding to $I = I_{lm}$ and measured at $T = T_j$.

C3D04060A: I_S(300 K) $\approx$ 1.47 $\times$ 10^{-17} A; C3D02060E: I_S(300 K) $\approx$2.14 $\times$ 10^{-17} A.

2.15. The calculation of A^*

Since we already calculated the values of parameters Φ_B, *S* and I_S, then the value of A^* can be obtained using (21a):

C3D04060A: $A^* \approx$68.1 A/(cm^2·K^2); C3D02060E: $A^* \approx$37.2 A/(cm^2·K^2).

2.16. Determination of overheating temperature of the SD chip active region

One can write the 2nd Kirchhoff law equation for an arbitrarily chosen point at the forward *I-V* characteristic of the diode:

$$V = V_T(T) + (I - I_{lm})R_d(T), \tag{24}$$

or:

$$V = V_T\left(T_j + \Delta T_h\right) + (I - I_{lm})R_d(T), \tag{24a}$$

where ΔT_h is the desired value of the overheating temperature.

For the practical application of (24) and (24a) one should know the function $V_T(T)$ which implies the dependence of diode forward voltage drop on the temperature at the constant forward current $I = I_{lm}$ [29]. If one has the set of forward *I-V* curves measured at different temperatures then each value of $V(T)$ can be found as the voltage coordinate of an intersection point between linearized section of each *I-V* curve (in the range of high currents) and the straight line $I = I_{lm}$. The information on $V_T(T)$ dependence may be given in the device datasheet [11,12].

The linearized $V(T)$ dependence has the form:

$$V_T(T) = V_0 - \alpha_T T, \tag{24b}$$

where V_0 is the value of V_T extrapolated to $T = 0$, α_T is the thermal sensitivity of the diode forward voltage drop at the constant current $I \approx I_{lm}$.

Inserting the expressions for V_T (24b) and R_d (2) into (24a) after corresponding transformations we obtain:

$$\Delta T_h = \frac{V - V_0 - R_0(I - I_{lm})}{\alpha_R(I - I_{lm}) - \alpha_T} - T_j, \tag{24c}$$

The values of ΔT_h of the diodes tested depending on the forward current flowing and voltage applied $I(V)$ at $T_j \approx$298 K in steady-state conditions are given in Table 2.

2.17. Plotting of a standard thermometric characteristic

A thermometric characteristic (TRC) of a diode or a diode sensor is the dependence of the diode forward voltage drop on the absolute temperature measured at low fixed current ($I \leq I_{lm}$). It is commonly accepted that "standard" TRC is the one that measured at $I = 10^{-5}$ A [19]. The TRC of structures based on 4H-SiC SD is distinguished by high linearity. In addition, the TRCs in the range of currents $I \leq I_{lm}$ are extrapolated down to the $T = 0$ point at one and the same voltage value V_0 [30–32] as a rule, i.e. they "converge into one point". These properties allow to plot the TRC using minimum number of experimental points (at least two) and to assess thermal sensitivity $s(I)$ of 4H-SiC SD operating as a temperature sensor [32,33] as well as maximum temperature value T_M to be measured by such a sensor. The TRC equation is:

$$V = V_0 - s(I)T \tag{25}$$

At $V = mkT/q$ [32] one can obtain the expression for T_M in the form:

$$T_M \approx \frac{qV_0}{mk + qs} \tag{25a}$$

"Standard" TRC parameters of the diodes tested:

C3D04060A: $V_0 \approx$1.33 V, $s(I \approx 10^{-5}$ A$) \approx$2.07 mV/K, $T_M \approx$617 K;

Table 2
Overheating temperature of the SD chip active region.

Device type	T_j, K	I, A (U, V)	ΔT_h, K
C3D04060A	298	10.0 (2.5)	~90.3
		10.0 (3.0)	159.1
C3D02060E	298	4.0 (2.45)	102.3
		4.0 (2.75)	166.1

C3D02060E: V_0≈1.44 V, $s(I≈10^{-5}$ A)≈2.55 mV/K, T_M≈545.2 K.

3. Application of the results obtained and its discussion

To check the values of electro-physical parameters obtained we shall apply the method of diode electrical characteristics calculation which has not been used in the modelling procedures in the Section 2. At the same time the values of electro-physical parameters and characteristics found in the Section 2 will be used as the initial data for such calculation. And we will compare the desired data to be calculated with the like given in the datasheets and the literature.

3.1. Diode constant forward current density (J_F)

$$J_F = \frac{I_F}{S}, \tag{26}$$

where I_F is the maximum value of constant forward current given in the device datasheet.

C3D04060A: $J_F \le 9.37$ A/mm^2 (~930 A/cm^2); C3D02060E: $J_F \le 7.27$ A/mm^2 (~720 A/cm^2).

These values are typical for Ni-4H-SiC SD and p-i-n diodes [34, $J_F \le 5{\cdot}10^3$ A/cm^2].

3.2. Maximum value of electric field intensity in the diode base layer (drift region), E_{max}

The value of E_{max} is determined by the following equation:

$$E_{max} \approx \frac{V_{DC}}{L_D}, \tag{27}$$

where V_{DC} is the blocking voltage given in the device datasheet, V.

C3D04060A: E_{max} ≈8.3 × 10^5 V/cm; C3D02060E: E_{max} ≈7.2 × 10^5 V/cm.

The values of E_{max} obtained are ~ 3 times lower than the critical value E_{cr}, calculated for the doping impurity concentration (1–5) × 10^{15} cm^{-3} in the samples of 4H-nSiC: E_{cr}≤(3–4) × 10^6 V/cm [16]. This corresponds to the electrical safety margin commonly accepted in the power semiconductor device engineering and ensures the device operation without avalanche initiation in its base region in the range of values $E \le E_{max}$.

3.3. Plotting of the diode reverse I-V characteristic

As the reverse voltage and temperature rise, the reverse *I-V* characteristic of the diodes investigated [11,12] becomes significantly different from the ideal one described by the expressions (21) and (21a) by a notable increase of the reverse current. In the work [31] it has been shown that in the range where reverse voltage is lower than the avalanche breakdown voltage, in high-voltage 4H-SiC SD the basic mechanism of reverse current rise dependent on the applied voltage and temperature is the potential barrier lowering caused by Schottky effect [15]. I. e. by the image force effect on the shape and height of Me-semiconductor potential barrier as well as by the presence of thin intermediate dielectric layer SiO_y between the metal and semiconductor. The voltage drop on this layer lowers the height of Me-semiconductor barrier [36]. Thus, the barrier height lowering value $\Delta\Phi_B$ is:

$$\Delta\Phi_B = \Delta\Phi_1 + \Delta\Phi_2, \tag{28}$$

where $\Delta\Phi_1$ is the value of potential barrier lowering related to the Scottky effect, $\Delta\Phi_2$ – caused by the intermediate layer influence. Here we have:

$$\frac{\Delta\Phi_1}{q} = \left(\frac{qE_{MS}}{4\pi\varepsilon_\alpha}\right)^{\frac{1}{2}}, \tag{29}$$

where E_{MS} is the value of maximum electric field intensity at the semiconductor's surface, which makes [9]:

$$E_{MS} = \sqrt{\frac{2qN_D V_R}{\varepsilon_\alpha}}, \tag{30}$$

V_R is the modulus of reverse voltage applied to the SD,

$$\frac{\Delta\Phi_2}{q} = \frac{\varepsilon_\alpha \delta E_{MS}}{\varepsilon_\delta + q\delta D_S}, \tag{31}$$

where D_S is the energy density of surface states corresponding to Fermi level in the metal, V^{-1}cm^{-2}; δ and ε_δ are the thickness and relative permittivity of the intermediate layer, correspondingly.

For SiC-based devices, the intermediate dielectric layer is considered to be thin, (see [36,35] and etc.) <1 μm thick native non-stoichiometric oxide SiO_y ($y < 2$) over the semiconductor surface (ε_δ≈2). Let us estimate a maximum thickness of this layer in the Mott's limit ($D_S \to 0$) according to the formula from the work [36]:

$$m \approx 1 + \frac{\delta\varepsilon_\alpha}{W_0(q\delta D_S + \varepsilon_\delta)}, \tag{32}$$

using the device structure parameters m and W_0 of the diode C3D4060A. Substituting numeric values into (32) we obtain that $\delta_{max} \le 30$ Å.

Using dependencies (20) and (20a) we can write the formula for reverse current I_R depending on V_R value as follows:

$$I_R = I_S exp\left(\frac{\Delta\Phi_B}{k_B T}\right)\left[1 - exp\left(-\frac{qV_R}{k_B T}\right)\right], \tag{33}$$

Here the value of $\Delta\Phi_B$ is determined by the relations (28)–(31), and the temperature-dependent parameter I_S, the saturation current at $T = T_j$ is found by the technique described in subsection 2.14 (see above).

In Fig. 5 one can see the dependence $I_R(V_R)$ of the diode C3D4060A measured at T_j≈175 °C (448 K) [12] (solid line). The result of reverse current calculation using relations (28)–(31), (33) and subsection 2.14 is marked by "x" in the figure. The parameters δ and D_S were chosen as adjustable ones (see (31)). In our case the best coincidence with the reverse *I-V* curve given in the device datasheet is achieved at δ≈10 Å (~2 monoatomic layers of SiO_y oxide, $\delta < \delta_{max}$) and D_S≈1 × 10^{13} V^{-1}cm^{-2} right down to V_R≈–970 V.

The results obtained are in satisfactory agreement with the data of works [35–37] and thus serve as one more proof of the adopted technique validity. Also we should note that the results of calculation of $I_R(V_R)$ dependence practically coincide with datasheet data and testify to a very good fit with the calculation data of electro-physical parameters of the active device diode structure (N_D, S, I_S, A^*, Φ_B, m and etc.) being

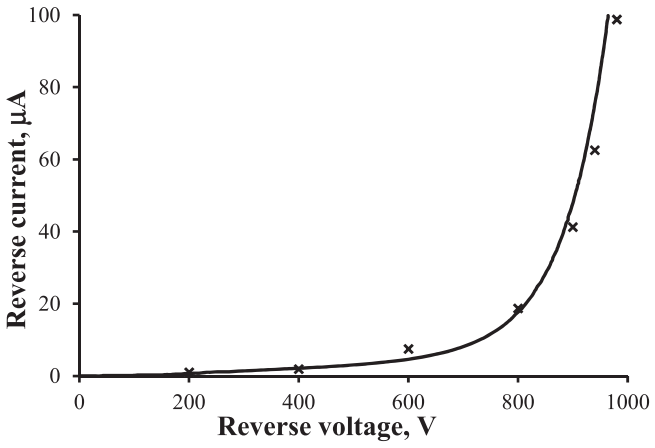

Fig. 5. Reverse characteristic $I_R(V_R)$ of the SD C3D04060A measured at T_j = 448 K: the calculation result is marked by "x" (δ≈10 Å, D_S≈1 × 10^{13} V^{-1}·cm^{-2}), solid curve has been taken from the Fig. 2 in ref. [12].

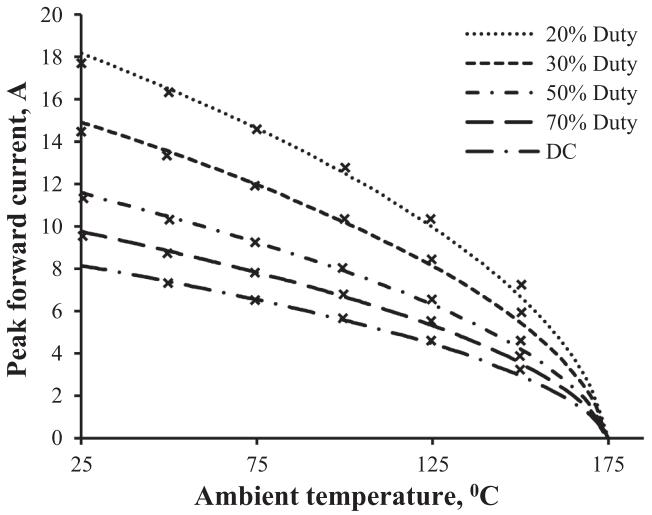

Fig. 6. Current derating curve (the dependence of peak forward current $I_{F(peak)}$ on the ambient temperature T_a and duty cycle n'): "x" is the calculation result by using (34), solid lines have been taken from the Fig. 3 in ref. [11].

used for the calculation of parameter I_R[b] directly or indirectly.

3.4. Determination of peak forward current dependencies on the ambient temperature and voltage pulse ratio

The following assumptions were used when deriving the computation formula:

- all the electric power is released within the diode n-base layer and the heat emission ability of the layer is much lower than the power released;
- thermal parameters of the diode design are such as when $T_j = 175$ °C (448 K) then $T_j = T_a$, where T_a is the ambient temperature, thus the power dissipated by the diode equals zero.

These assumptions are in agreement with the data from the diodes datasheets: Fig. 6 [11] and Fig. 4 [12]. To calculate the peak forward current ($I_{F(peak)}$) dependencies on the ambient temperature T_a and the supply voltage pulse ratio, the following formula was obtained from the heat equilibrium condition:

$$I_{F(peak)} = \left[\frac{2f_{l.l.}c\rho L_D S(T_{jmax} - T_a)}{n' R_d(T_{jmax})}\right]^{\frac{1}{2}}, \tag{34}$$

where $f_{l.l.}$ is the lower limit of the supply voltage pulse frequency, specific for each device type[c], c is the heat capacity and ρ is the density of a semiconductor material in the base layer of the SD, $T_{j\ max}$ is maximum value of the junction temperature given in the device datasheet, n' is the duty cycle of supply voltage pulses.

Approving of the dependence (34) was done for SD C3D02060E [11]. The values of initial parameters were as follows: $T_{j\ max} \approx 175$ °C (448 K) [11], $c = 690$ J/(kg × K) and $\rho \approx 3.21 \times 10^3$ kg/m^3 [24]. In this case the value of $f_{l.l.}$ makes ~ 5.37 kHz (the standard supply voltage pulse ratio equals 2) The requirement for $f_{l.l.}$ value (above 1 kHz) given in [11] is met with excess. The calculation results are shown in Fig. 6. The calculated values (separate points) in the whole range of temperatures T_a and n' values demonstrate good match with the curves (solid lines) taken from the device datasheet [11].

3.5. The total charge of electrons removed from the base area depending on the reverse voltage

The value of this charge (Q_C) is adequately described by the trivial equation [2]:

$$Q_C = S\sqrt{2q\varepsilon_a N_D V_R}, \tag{35}$$

which is valid in the conditions of total ionization of a donor impurity in the diode base area.

The corresponding dependence calculated for the diode C3D04060A is given in Fig. 7 (separate points). The solid line in the figure corresponds to the curve taken from the datasheet [12]. As it can be seen in the Fig. 7, the coincidence of calculated and experimental values of Q_C is observed up to the reverse voltage magnitude ~ 500–550 V.

At higher values of the reverse voltage there is some discrepancy between the calculation and experimental data which increases monotonically as the reverse voltage rises. This could be connected with the increase of electron concentration n above the $n = N_D$ value at the expense of both: the field ionization of traps as well as the injection mechanisms considered, for example, in [38]. We should note that the study of this issue is out of the purpose frameworks of the present work and could be the subject of a separate investigation being important for the practical applications.

3.6. Modelling of the capacitance stored energy (E_{cap}) dependence on the reverse voltage value (V_R), applicable to SD

The dependence $E_{cap}(V_R)$ obeys the following apparent equation:

$$E_{cap} = \frac{\varepsilon_a S}{2L_D} \bullet V_R^2, \tag{36}$$

The modelling result for SD C3D04060A is shown in Fig. 8. Here separate points are the result of calculation; solid curve corresponds to the curve in Fig. 7 of the datasheet [12]. Fig. 8 shows that there is a good fit between calculation and experimental data which testify to the reliability of electro-physical parameters S and L_D calculated for SD C3D04060A.

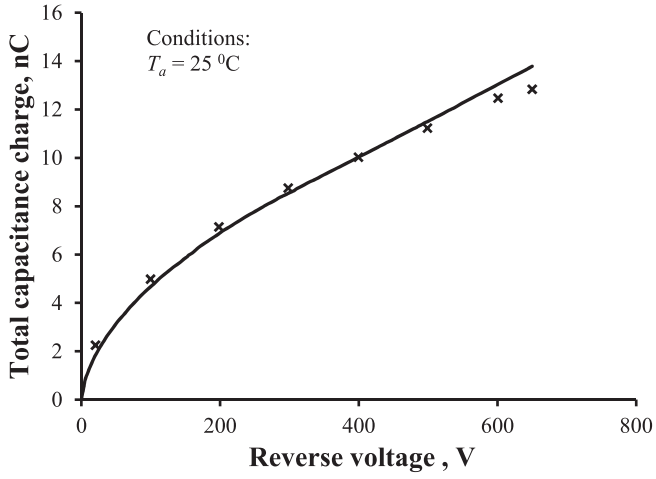

Fig. 7. Total capacitance charge (Q_c) vs. reverse voltage (V_R) for C3D04060A: "x" is the calculation result, solid curve has been taken from the Fig. 5 in ref. [12].

[b] Note that the simulation and calculations of the dependence $I_R(V_R)$ for C3D02060E diode have resulted in similar results. Thus they are not presented separately.

[c] If the signal frequency is lower than this value, then n'=1 and thus the dependence $I_{F(peak)}(T_a, n')$ is reduced to the direct current case.

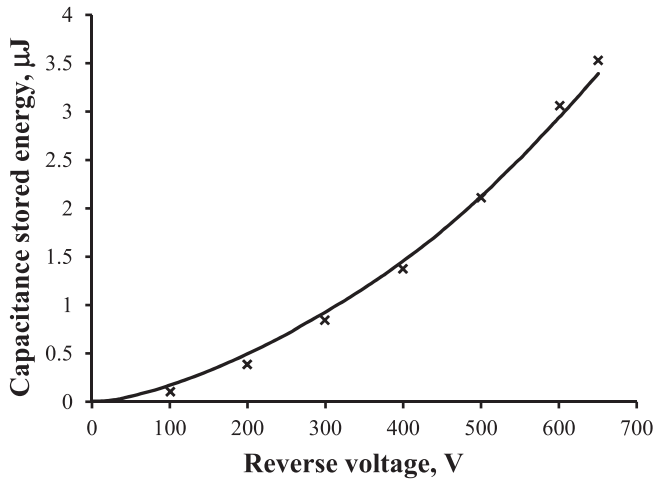

Fig. 8. Capacitance stored energy E_{cap} vs. V_R (C3D04060A): "x" is the calculation result; solid curve has been taken from the Fig. 7 in ref. [12].

3.7. Determination of maximum electron drift velocity ν_{sm} in the SD base

Charge carrier drift velocity is an important parameter of a semiconductor material. In particular, the electro-physical parameter ν_{sm} limits the value of such a key electrical parameter of SD as non-repetitive peak forward surge current [11,12]. We can assess the value of ν_{sm} using the following simple relation:

$$\nu_{sm} = \frac{J_{spm}}{q(N_D + \Delta n)}, \tag{37}$$

where J_{spm} is the maximum value of the current density in the SD base area,

$$J_{spm} = \frac{I_{Fmax}}{\sqrt{2S}}, \tag{37a}$$

I_{Fmax} is the non-repetitive peak forward surge current; Δn is the concentration of excessive electrons connected, in particular [21], with monopolar electron injection into n-layer of the device structure from heavily doped n^+-layer (Fig. 1). According to the estimations in [21], usually for such SD the value $\Delta n < 1{\cdot}10^{14}$ cm^{-3} thus it can be neglected during the calculations using (37).

The calculation results of ν_{sm} for the diodes investigated are as follows:

C3D04060A: ~1.52×10^7 cm/s at the electric field intensity ~ 3.1×10^5 V/cm;

C3D02060E: ~1.31×10^7 cm/s at the electric field ~ 7.83×10^4 V/cm. In our opinion, the value of $I_{FSM} = 65$ A given in the datasheet of the diode C3D02060E [11] is underrated, at least by ~ 10% of the value.

We should note that these values are close enough to the values of saturated drift velocity of electrons (~1.55×10^7 cm/s at the field intensity above 2×10^5 V/cm) obtained in the work [21] for the samples 4H-SiC SD. So one can consider that the values of S, L_D, and N_D correspond to the real value of saturated drift velocity of electrons in 4H-SiC semiconductor material (along c axis in the fields $\geq 2 \times 10^5$ V/cm) and, therefore, correlate with the values of I_{Fmax} [12] and I_{FSM} [11].

Table 3 shows the parameters of SD C3D04060A extracted by using the procedure described in [5] as well as by our technique proposed.

(a) – the empirical assumption, (b) – recalculation for $I = 4$ A, (c) – our calculation using parameters from [5].

Analyzing Table 3 one can see that the orders of magnitude of parameters extracted in this work are close to those obtained in the work [5]. In our opinion the discrepancy observed is due to the choice of μ_n(300 K), m and A^* values as basic ones by the authors in [5] instead of extracting them from simulation and/or experiment. But according to our method almost all the parameters are calculated using the initial information from datasheets and direct measurements.

Thus the calculation results of the SD electrical parameters carried out in this section allow to conclude that the electro-physical parameters calculated in the Section 2 (S, L_D, N_D, I_S, m, A^*, Φ_B and etc.) are in very good agreement with the experimental (rated) electrical parameters of the commercial diodes [11,12]. (The parameter μ_n(300 K) as well as $\mu_n(T)$ dependence should be placed here as well since the calculations of N_D, μ_n(300 K) and $\mu_n(T)$ are interrelated and self-consistent.) Therefore, the express technique of SD electro-physical parameters calculation developed in this work demonstrated its practical value.

For a commercial or experimental diode chosen the parameter extraction procedure may be realized by executing the following steps:

1. Assumptions:
   - isothermal I-V characteristics of the diode are approximated by straight lines (1) at high currents and the dependence $R_d(T)$ obeys equation (2);
   - the dependence $\mu_n(N_D$, 300 K) is described by equation (7) and temperature dependence $\mu_n(T)$ – by equation (11);
   - the intrinsic conductivity state criterion: $n_i(T_i) = 0.1N_D$.
2. Measurements:
   - C-V characterization of the diode at the reverse bias (subsection 2.3) if there are no C-V curves in the datasheet or the datasheet is absent itself;
   - I-V characterization of the forward biased diode at the low current and $T = 300$ K (see subsection 2.12).
3. Determine the $R_d(T)$ dependence according to subsection 2.2.
4. Determine the values of C_{PT} and V_{PT} using C-V characteristics according to subsection 2.4.
5. Calculate the value of N_D according to subsection 2.5.
6. Calculate the value of μ_n(300 K) according to subsection 2.6.
7. Calculate the value of T_i and plot $\mu_n(T)$ dependence following the instructions in subsections 2.7 and 2.8.
8. Calculate the values of L_D and S using the equations from subsections 2.9 and 2.10.
9. Calculate the value of diffusion potential V_{bi} of Me-semiconductor junction using equations (17) and (18a), subsection 2.11.
10. Calculate the value of Φ_B according to subsection 2.12.
11. Calculate the value of I_S by following the instructions in subsections 2.13 and 2.14.
12. Determine the value of A^* according to subsection 2.15.
13. Determine the value of ΔT_h according to subsection 2.16 (also at different currents and/or voltages given).
14. Plot the standard thermometric curve of the diode (subsection 2.17) with calculation of s and T_M at $I = $ const., $I = 10^{-5}$ A.
15. Determine the value of diode constant forward current density (J_F), subsection 3.1.
16. Calculate the maximum value of electric field intensity, E_{max}, in the diode drift region, subsection 3.2.
17. Plot the reverse diode I-V characteristic by following the instructions in subsection 3.3.

Table 3
Comparison of the SD parameters extracted by two different methods.

Parameter	N_D, cm^{-3}	L_D, μm	S, mm^2	Φ_B, eV	x	μ_n(300 K), cm^2/V·s	m	A^*, A/cm^{2}K^2	J_F, A/cm^2	E_{max}, V/cm	V_{sm}, cm/s
Technique used in [5]	2.97×10^{15}	7.37	2.2	1.2	1.4	500[(a)]	1.0[(a)]	146[(a)]	180.51	1.02×10^6	1.49×10^7[(c)]
Present work	4.45×10^{15}	7.0	1.44	1.3	1.64	875	1.02 ÷ 1.03	68.1	277.8[(b)]	8.3×10^5	1.52×10^7

18. Determine the values of $I_{F(peak)}$ using equation (34), subsection 3.4.
19. Plot the dependence of the total charge of electrons removed from the base area on the diode reverse voltage, subsection 3.5.
20. Plot the dependence $E_{cap}(V_R)$ according to subsection 2.16.
21. Determine the value of maximum electron drift velocity in the diode base area, subsection 3.7.

4. Conclusion

The method proposed for the calculation of a series of basic electrophysical parameters of the power SD is based on the device characteristics given in the datasheets as well as on performing the required ordinary *I-V* and/or *C-V* characterizations of the device. The method does not require any additional information on the technological processes of device fabrication, in other words it is based exceptionally on the physical model application.

Unlike the well-known calculation procedures of the SD electrophysical parameters (see, for example, [5] and others) our technique does not use empirical assumptions for certain parameters and minimally operates with the data of processing of device electro-physical characteristics presented graphically. This allows to decrease significantly the absolute error of the SD electro-physical parameters determination and to increase its reliability. (The model and calculations in [5] are based on the assumption that the numerical value of low-field mobility of the majority charge carriers is already known. This narrows essentially the scope of such a technique, in particular.)

The approval of the values of electro-physical parameters obtained is based on the complex calculation of the nominal device electrical parameters and characteristics given in the datasheet as well as on establishing the proper correlation between the calculated parameters and performance characteristics. Therefore the technique profitably differs from the known procedures in our opinion. For the first time the calculation of thermometric characteristics and parameters of devices was introduced into the procedure of commercial power SD parameter extraction. This promotes the expansion of SD application range into the field of diode thermometry. Despite the fact that the technique proposed was tested for the Schottky diode parameter extraction, it can be applied to the parameter extraction procedure of power p^+-n_0-n^+ diodes based on SiC being actively developed in recent years. And, unlike many well-known similar methods, it allows to determine the parameters of diode operation in pulsed mode.

The results of this work could be useful for both: semiconductor device developers and application specialists dealing with such devices. In addition, the approach adopted in this work to the determination and verification of SD electro-physical parameters if combined with $\mu_n(T)$ dependence investigations [21, 22 and others] could, in our opinion, become a basis for the development of phenomenological theory of operation of power SDs and p-i-n diodes in the range of high temperatures.

Declaration of Competing Interest

The authors declare that they have no known competing financial interests or personal relationships that could have appeared to influence the work reported in this paper.

References

[1] Kimoto T, Cooper JA. Fundamentals of silicon carbide technology: growth, characterization, devices and applications. John Wiley & Sons Singapore Pte. Ltd.; 2014.
[2] Ivanov PA, Grekhov IV, Il'inskaya ND, Kon'kov OI, Potapov AS, Samsonova TP, et al. High-voltage (3.3 kV) 4H-SiC JBS diodes. Semiconductors 2011;45:668–72.
[3] Rottner K, Frischholz M, Myrtveit T, Mou D, Nordgren K, Henry A, et al. SiC power devices for high voltage applications. Mater Sci Eng, B 1999;61–62:330–8.
[4] Grekov AE, Chen Z, Fu R, Hudgins JL, Mantooth HA, Sheridan DC, et al. Parameter extraction procedure for vertical SiC power JFET. IEEE Trans Ind Appl 2011;47:1862–71.
[5] Fu R, Grekov AE, Peng K, Santi E. Parameter extraction procedure for a physics-based power SiC Schottky Diode model. IEEE Trans Ind Appl 2014;50:3558–68.
[6] Wang Hao, Chen Xing, Xu Guang-Hui, Huang Ka-Ma. A novel physical parameter extraction approach for Schottky diodes. Chin. Phys. B 2015;24:077305.
[7] Ortiz-Conde A, García-Sánchez FJ. A new approach to the extraction of single exponential diode model parameters. Solid State Electron 2018;144:33–8.
[8] Ocaya RO. A current–voltage–temperature method for fast extraction of schottky diode static parameters. Measurement 2014;49:246–55.
[9] Helal H, Benamara Z, Pérez BG, Kacha AH, Rabehi A, Wederni MA, Mourad S, Khirouni K, Monier G, Robert-Goumet C. A new model of thermionic emission mechanism for non-ideal Schottky contacts and a method of extracting electrical parameters. Eur Phys J Plus 2020;135. Art.No.895.
[10] Yin S, Gu Y, Tseng KJ, Li J, Dai G, Zhou K. A physics-based compact model of sic junction barrier schottky diode for circuit simulation. IEEE Trans Electron Devices 2018;65:3095–103.
[11] C3D02060E datasheet. https://www.wolfspeed.com/downloads/dl/file/id/116/product/653/c3d02060e.pdf (accessed Feb. 22, 2021).
[12] C3D04060A datasheet. https://www.wolfspeed.com/downloads/dl/file/id/845/product/653/c3d04060a.pdf (accessed Feb. 22, 2021).
[13] Alexandrov P, Zhao JH, Wright W, Pan M, Weiner M. Inductively-loaded half-bridge inverter characterisation of 4H-SiC merged PiN/Schottky diodes up to 230 A and 250 °C. Electron Lett 2001;37:1261. https://doi.org/10.1049/el:20010850.
[14] Hefner A, Berning D, Lai JS, Liu C, Singh R. Silicon carbide merged PiN Schottky diode switching characteristics and evaluation for power supply applications. In: Proc. 35th IAS Ann. Meet. & World Conf. on Ind. Appl. of Electr. Energy, IEEE (2000) Rome, Italy, 2948–2954.
[15] Sze SM, Ng KK. Physics of semiconductor devices. 3rd ed. Hoboken, NJ, USA: John Wiley & Sons, Inc.; 2007.
[16] Baliga BJ. Silicon carbide power devices. Singapore: World Scientific Publishing Pte. Ltd.; 2005.
[17] Kannam PJ. Design concepts of high energy punchthrough structures. IEEE Trans Electron Devices 1976;23:879–82.
[18] Ivanov PA, Grekhov IV, Potapov AS, Samsonova TP, Il'inskaya ND, Kon'kov OI, et al. Excess leakage currents in high-voltage 4H-SiC Schottky diodes. Semiconductors 2010;44:653–6.
[19] Dodrill BC, Krause JK, Swinehart PR, Wang V. Performance characteristics of silicon diode cryogenic temperature sensors. In: Kelley JP, editor. Applications of cryogenic technology. Boston, MA, USA: Springer; 1991. p. 85–107.
[20] Schubert EF. Light-emitting diodes. 2nd ed. New York, NY, USA: Cambridge University Press; 2006.
[21] Ivanov PA, Potapov AS, Samsonova TP, Grekhov IV. Field dependence of the electron drift velocity along the hexagonal axis of 4H-SiC. Semiconductors 2016;50:883–7.
[22] Schaffer WJ, Negley GH, Irvine KG, Palmour JW. Conductivity Anisotropy in Epitaxial 6H and 4H SiC. In: Proc. MRS symp., vol. 339, San Francisco, CA, USA; 1994, p. 595–600.
[23] Kulish NR, Shwarts YM, Borblik VL, Venger YF, Sokolov. VN. Self-consistent method for optimization of parameters of diode temperature sensors. Semiconductor Phys Quantum Electron Optoelectronics 1999;2:15–27.
[24] For information on materials properties see: http://www.matprop.ru/SiC_bandstr (accessed Feb. 22, 2021).
[25] Matthus CD, Di Benedetto L, Kocher M, Bauer AJ, Licciardo GD, Rubino A, et al. Feasibility of 4H-SiC p-i-n diode for sensitive temperature measurements between 20.5 K and 802 K. IEEE Sens J 2019;19:2871–8.
[26] Shalimova KV. Fizika poluprovodnikov (Physics of Semiconductors). St. Petersburg, Russia: Lan'; 2010 (in Russian).
[27] Raynaud C, Isoird K, Lazar M, Johnson CM, Wright N. Barrier height determination of SiC Schottky diodes by capacitance and current-voltage measurements. J Appl Phys 2002;91:9841–7.
[28] Krasnov VA, Shwarts YM, Shwarts MM, Kopko DP, Yerochin SY, Fonkich AM, et al. Investigation of thermometric characteristics of p^+-n-GaP diodes. Technol Design Electron Equipment 2008;6:38–40 (in Russian).
[29] Demenskyi OM, Yerochin SY, Krasnov VA, Shutov SV. Determination of the overheating temperature of SiC power Schottky diodes. In: Proc. FEE::2016, Sumy, Ukraine, p. 159. (in Russian).
[30] Draghici F, Badila M, Brezeanu G, Rusu I, Craciunoiu F, Enache I, et al. An industrial temperature probe based on SiC diodes. In: Proc. CAS 2010 (IEEE), Sinaia, Romania; 2010. p. 409–12.
[31] Demenskiy AN, Yerochin SY, Krasnov VA, Shutov SV. High-temperature sensors based on 4H-SiC Schottky diode structures. In: Reports of Int. Youth Conf. (PhysicA SPb/2015), St. Petersburg, Russia, p. 90–92. (in Russian).
[32] Krasnov VA, Shutov SV, Yerochin SY, Demenskyi OM. High temperature operation limit assessment for 4H-SiC Schottky diode-based extreme temperature sensors. IEEE Sens J 2019;19:1640–4.
[33] Josan I, Boianceanu C, Brezeanu G, Obreja V, Avram M, Puscasu D, Ioncea A. Extreme environment temperature sensor based on silicon carbide Schottky diode. In: Proc. of 2009 Int. Semicond. Conf. (IEEE), Sinaia, Romania, p. 525–528.
[34] d'Alessandro V, Irace A, Breglio G, Spirito P, Bricconi A, Carta R, Raffo D, Merlin L. Influence of Layout Geometries on the Behavior of 4H-SiC 600V Merged PiN Schottky (MPS) Rectifiers. In: Proc. 18th Int. Symp. Power Semicond. Dev. & IC's, Naples, Italy, 2006; p. 1–4.

[35] Ivanov PA, Grekhov IV, Kon'kov OI, Potapov AS, Samsonova TP, Semenov TV. I-V characteristics of high-voltage 4H-SiC diodes with a 1.1-eV Schottky Barrier. Semiconductors 2011;45:1374–7.
[36] Rhoderick EH, Williams RH. Metal-semiconductor contacts. 2nd ed. Oxford, England: Clarendon Press; 1988.
[37] Nicholls J, Dimitrijev S, Tanner P, Han J. Description and verification of the fundamental current mechanisms in silicon carbide Schottky barrier diodes. Sci Rep 2019;9:3754.
[38] Lampert MA, Mark P. Current injection in solids. New York, London: Academic Press; 1970.

Vasily A. Krasnov graduated from Odessa polytechnic institute in 1973. He received his Ph.D. in Electronic Engineering from Kiev institute of semiconductors, Academy of Sciences of Ukrainian republic in 1987. Currently he is a senior researcher with Laboratory N10-2 "Technology of Materials for Optoelectronics" in V. Lashkaryov Institute of Semiconductor Physics, National Academy of Sciences, Ukraine. The basic area of his research and development activity is connected with physics and technology of semiconductor devices and active device structures.

Sergey Yu. Yerochin received his B.Sc. degree in Electronics in 1998 and M.Sc. degree in Materials Science and Engineering in 1999 from Kherson National Technical University. Currently he is a researcher with Laboratory N10-2 "Technology of Materials for Optoelectronics" in V. Lashkaryov Institute of Semiconductor Physics of National Academy of Sciences, Ukraine. His main research interests are focused on obtaining III-V semiconductor heterostructures and thin films, measurement and characterisation of high-temperature and power semiconductor devices, wide bandgap temperature sensors.

Oleksii M. Demenskyi received his B.Sc. degree in Energetics in 2008 and M.Sc. degree in Renewable energy sources in 2009 from Kherson National Technical University. From 2009 to 2012 he has been a Ph.D. student of V. Lashkaryov Institute of Semiconductor Physics of National Academy of Sciences, Ukraine. Currently he is a junior researcher with Laboratory N10-2 "Technology of Materials for Optoelectronics" in V. Lashkaryov Institute of Semiconductor Physics, NASU. His main research interests are: alternative energy and energy saving technologies, semiconductor devices, sensors development.